

Implosion of indirectly driven reentrant cone shell target

R.B. Stephens,¹ S.P. Hatchett,² R.E. Turner,² K.A. Tanaka,³ and R. Kodama³

¹*General Atomics, San Diego, CA, USA 92186, USA*

²*Lawrence Livermore National Laboratory, Livermore, CA 94550, USA*

³*Institute for Laser Engineering, Osaka University, Osaka, JAPAN*

Abstract. We have examined the implosion of an indirectly driven reentrant-cone shell target to clarify the issues attendant on compressing fuel for a Fast Ignition target. The target design is roughly hydrodynamically equivalent to a NIF cryo-ignition target, but scaled down to be driven by Omega. A sequence of backlit x-radiographs recorded each implosion. The collapse was also modeled with LASNEX, generating simulated radiographs. We compare experimental and simulated diameter, density and symmetry as functions of time near stagnation. The simulations were generally in good agreement with the experiments with respect to the shell, but did not show the pre-stagnation central absorption maximum. The existence of material between the original cone and the shell is sensitive to gold M-band radiation, from laser spots, which penetrates the shell and ablates gold from the cone. The simulated radiographs using recently measured M-band fractions showed absorption between the cone and shell similar to the experiment. This gold ablation might be a problem in a cryo-ignition target.

PACS Nos:

I. Introduction

The Fast Ignition (FI) Inertial Fusion Energy (IFE) concept is recognized as having the potential to improve the attractiveness of IFE reactors. FI ignites the dense core of separately compressed fuel pellets with a very intense laser pulse [1], achieving much higher gain than is possible with the baseline central hot spot approach [2]. Realization of this concept is somewhat complicated because the target core (~ 200 g/cc) is hidden under a plasma corona that is opaque for densities higher than ~ 0.01 g/cc. A FI IFE target therefore must allow the possibility of efficiently converting the photons to a beam of charged particles that deposit their energy in a localized volume of the assembled core. In the initial conception, a laser pre-pulse was used to clear a path deep into the plasma and allow the ignition pulse to penetrate close to the core [3], where it could create a spray of \sim MeV electrons. Experiments have shown efficient conversion to electrons [4], and tunnel digging [5], but it seems difficult to extend the digging sufficiently to get close to a very dense core. An alternative to ponderomotive tunneling is the use of a reentrant cone to exclude the plasma blowoff from one sector of the target; this allows the ignition laser a clear, close approach to the assembled core, and a controlled surface at which to create the electrons [6].

Targets of this form are extremely anisotropic. It is a question whether one could assemble a usable core from such a geometry; or even whether existing hydro models, which accurately describe the implosion of nearly symmetric targets, could accurately predict the implosion of a reentrant-cone-in-shell target. The presence of the reentrant cone near the core could cause turbulence, preventing a useful assembly of fuel, or cause contamination, preventing the assembled fuel from burning.

We set out to examine those questions; the purpose of this paper is to compare the experimental and modeled behavior of an indirect drive, reentrant-cone-in-shell target. The results of our experiment show that the target hydro is well modeled by standard

codes, and the fuel is assembled in a reasonably compact form close to the density and form predicted by the simulation. However, some of the indirect drive spectrum (that from the non-thermal M-line emissions from the gold hohlraum) penetrates the shell and generates vapor from the surface of the gold cone. Turbulent mixing at the CH/Au interface apparently allows some gold vapor to mix into the low density center of the assembling target. Future target designs should incorporate cone designs that minimize the generation of high-Z contaminant, or should use direct drive.

II. Experiment

A cross-section of the target design is shown in Fig. 1(b). It was scaled from the 1.8 MJ NIF ignition target in Fig. 1(a) to be driven with 14 kJ in a scale 1 hohlraum on Omega. The shell is 510 μm od with a 57 μm thick plasma polymer wall. The cone is \sim 30 μm thick Au with a hyperboloidal tip (foci separation 40 μm) and a 35 deg. half angle* the tip is 20 μm from the intersection of the asymptotes, and that is 12 μm from the center of the shell. The cone was attached to the shell with UV curing glue. This assembly was mounted in a hohlraum that had backscatter windows orthogonal to the hohlraum and cone axes (Fig. 2). The gold cone was stepped to minimize interference with adjacent high angle laser beams, and to avoid creating hot spots on the cone surface close to the shell; either effect would have distorted the drive. Forty drive beams were oriented as for a standard indirect drive shot and driven using pulse shape 26, a \sim 3 ns long shaped pulse that is standard for high-convergence indirect drive targets [7].

We used Fe (6.7 keV for He-like Fe) illuminated by 20 beams to backlight the target for an x-ray framing camera that took images through a 10 μm pinhole at \sim 70 ps intervals. The fixed structure in the images was eliminated by reference to a flat-field image (*i.e.* camera was illuminated with an open aperture instead of a pinhole) [8]. One pixel wide streaks in the image, from pixel defects, were replaced with the adjacent row of pixels. Then the images were smoothed using a 5 μm boxcar average.

This sequence of pictures clearly shows the evolution of the shell and cone [Fig. 3(a) – only every other image is shown]. Two equivalent (including pixelation, time-smearing, and smoothing) sets of pictures were generated from LASNEX [9] simulations of the implosion [Figs. 3(b,c)]. The first simulation set used an estimated M-band fraction (the energy fraction of incident x-rays in the band from 2-5 keV) that peaked at 4% at the peak of the pulse. This was consistent with best estimates at the time of the experiments. Recent (Spring 2003) measurements of the M-band fraction in hohlraums driven similarly are in the 6%-9% range at the peak [10]. The second simulation set uses 6% at the peak, but the same overall incident flux vs. time as the first set. From the image sets profiles were taken from a 15 μm wide, 300 μm long strip perpendicular to the cone axis. Backlighter brightness along that path was estimated by fitting a parabola to the intensity seen at each end of the strip. Experimental dark counts were estimated from counts between illuminated sections.

Using the brightness and background, we calculate the x-ray optical depth vs. position across the apparent center of each image for both the experimental and simulated images (Fig. 4), the full width half density size of the assembled target as a function of time (Fig. 5).

III. Discussion

Comparing the experimental and simulated radiographs, one sees that the collapsing shell's apparent stagnation time (3.3 ns), fwhm size (70 μm), and maximum x-ray optical depth (2), agree with the model (3.4 ns, 65 μm , and 2, respectively), the gross structure of the collapsing shell (horseshoe crab-like) looks very much as predicted, and we assembled about the expected fraction of the mass ($m/m_o = 28 \pm 4\%$ – calculated from the lineouts ignoring the cone and assuming spherical symmetry to the collapsing mass). But there are differences: the experimental profiles lack the shallow hollow in the center and increasing optical depth at early times that ought to be observable (Fig. 4), and an

associated decreasing fwhm during shell collapse (Fig. 5). More noticeably, the apparent cone shadow extends close to the shell in a manner inconsistent with the lower M-band fraction simulations. We believe these effects are connected. Most of that shadow is merely dense vapor [Fig. 6(b)]. The very opaque region (solid gold) is marked off by the white line in Fig. 6(b); the rest of the shadow transmits a few to 10% of the backlight (~ 1 g/cc of Au). The model x-ray drive included the non-thermal M-line radiation from the gold hohlraum, with peak fractions of 4% and 6% as described earlier [Figs 3(b,c)]. In the simulations these high energy x-rays penetrate the capsule and heat the tip of the cone, causing ablated gold plasma to extend past the center of the collapsing shell as seen in the experiment [Fig. 6(a)]. Later, as the capsule collapses, plastic plasma blown off the inside of the shell by shock waves impinges on the gold plasma with a pressure gradient that tries to push the gold plasma back toward the cone tip, but the Au vapor is dense enough that the boundary is Rayleigh/Taylor unstable some of the time, so some mixing is expected. This instability, however, is *not* captured by our simulations because it was not feasible to provide sufficient resolution in that region of these full implosion simulations. Therefore, in the simulations the gold plasma *is* pushed back with the result that no gold opacity remains in the capsule core region after ~ 3 ns. In reality we expect the interface to be quite perturbed with the result that some gold plasma would not be pushed back toward the cone and out of the core but would instead be mixed with the plastic plasma in the interface region resulting in the core opacity seen in the experiment. Consider Fig. 4(b), roughly peak convergence. There is an optical depth deficit in the simulations, with respect to the experiments, of about 0.3 over the central 30 microns. Using a gold opacity of about $327 \text{ cm}^2/\text{g}$ at 6.7 keV,** we find this deficit corresponds to about 4 ng of gold, amounting to about 1% of the mass density over that 30 micron diameter. That gold, in the larger cavity could also explain the unexpectedly high early time absorption seen in Fig. 4(a). The observed central optical depth could be due to C in

the central volume caused by turbulent mixing, but that requires an unusually high central density (~ 25 g/cm 3) at early time – about the same as observed at maximum compression.

The 4 ng of gold estimated above is roughly 0.04 wt% of the collapsed mass, and therefore must be considered as a potential problem for ignition. At ignition scale, 0.1 wt% of gold is sufficient to double the required ignition energy. Clearly, the amount of gold plasma ablated is sensitive to the amount of penetrating M-band radiation, but it seems difficult to eliminate this non-thermal, hard x-ray source since all the alternative hohlraum materials and mixtures (“cocktail hohlraums”) have fluorescent lines in the range 1-4 keV. At ignition scale, the shielding against those lines is much better; a NIF scale shell would have a doped ablator wall (~ 100 microns of Be:Cu0.02) that has ~ 5 times the 2 keV absorption length.

Mixing of ablated gold into the central core (which could be quite detrimental to full scale FI) should not occur if the capsule is directly driven. An experimental test of this hypothesis is currently being undertaken.

IV. Conclusion

The presence of the reentrant cone causes gross changes in the collapse that are reasonably well described by LASNEX modeling; this suggests that the hydro-equivalent, NIF scale, cryo-ignition target would implode to a useful ρR . However, non-thermal emissions from the gold hohlraum vaporized gold off the outside of the reentrant cone, and this vapor apparently mixed into the low density core of the assembled fuel. This contamination is potentially serious for indirect drive; adding 0.1 wt% Au doubles the required ignition energy. Alternatively, using direct-drive geometry [11,12] would avoid the problem entirely.

Acknowledgment

This work was performed under the auspices of the U.S. Department of Energy under Contract No. DE-FG03-00SF2229, by the University of California, Lawrence Livermore National Laboratory under Contract No. W-7405-Eng-48, and with the additional corporate support of General Atomics. The authors gratefully acknowledge the fabrication by J. Smith and assembly by S. Grant of the complex targets used for these experiments. We are indebted to the Omega team for operational support.

References

- * hyperboloidal shape was chosen for modeling convenience
- ** the simulation indicates that the core is heated to \sim 400 eV, which strongly bleaches the C absorption there, but has little effect on the Au

- [1] M. Tabak, et al., *Phys. Plasmas* **1**, 1626 (1994).
- [2] M. Rosen, *Phys. Plasmas* **6**, 1690 (1999).
- [3] A. Pukhov and J. Meyer-ter-Vehn, *Phys. Rev. Lett.* **79**, 2686 (1997).
- [4] M.H. Key, et al., *Phys. Plasmas* **5**, 1966 (1998).
- [5] A.J. Mackinnon, et al., *Phys. Plasmas* **6**, 2185 (1999).
- [6] M. Tabak, E.M. Campbell, J.H. Hammer, W.L. Kruer, M.D. Perry, S.C. Wilks, and J.G. Woodworth, Lawrence Livermore National Laboratory Patent Disclosure, IL-8826B, 1997, Lawrence Livermore National Laboratory, Livermore CA.
- [7] P. Amendt, R.E. Turner, and O.L. Landen, *Phys. Rev. Lett.* **89**, 165001 (2002).
- [8] O.L. Landen, et al., *Rev. Sci. Instrum.* **72**, 627 (2001).
- [9] J. Harte et al., *1996 ICF Annual Report*, Lawrence Livermore National Laboratory, Livermore CA, UCRL-LR-105821-96, 150 (1997). Available online at <http://www.llnl.gov/tid/lof/documents/pdf/233052.pdf>.
- [10] P. Amendt and R.E. Turner, unpublished.
- [11] R. Kodama, et al., *Nature* **412**, 798 (2001).
- [12] R. Kodama, et al., *Nature* **418**, 933 (2002).

List of Figure Captions

Figure 1. (a) A NIF scale cryogenic ignition target consisting of a 2 mm o.d. Be shell surrounding a DT ice layer, into which a hyperboloidal cone is inserted. (b) Cross section of shell in (a) scaled down for OMEGA experiments.

Figure 2. Schematic of reentrant cone-in-shell target mounted in an Omega scale 1 hohlraum. The 7 μm thick Cu backscatterer foil is mounted on the hohlraum wall behind the shell; the x-ray framing camera looks at the target from the other side through a 50 μm thick CH window with 0.15 μm thick Ta coating on the inside.

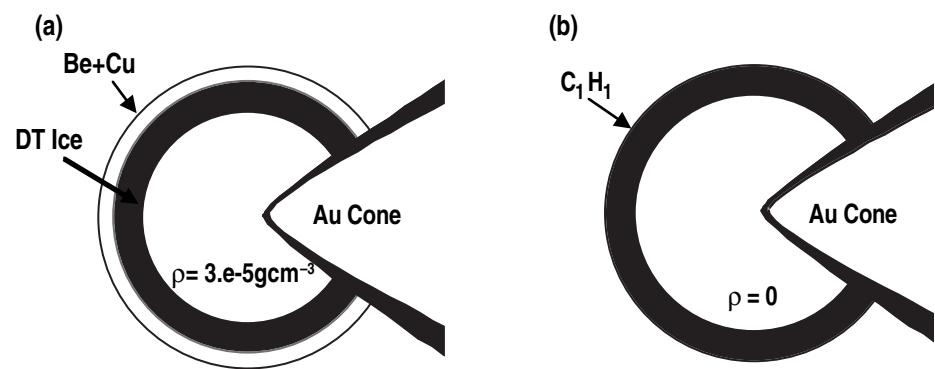
Figure 3. X-radiograph sequence of shell collapse (a) experimental results, (b) simulated collapse sequence at 140 ps intervals using 4% max in the gold M-line emission spectrum, (c) simulated collapse using 6% max in the gold M-line emission spectrum. The stagnation points (the *ed images — 3.33 and 3.4 ns for experiment and simulations, respectively) are set under one another.

Figure 4. Comparison of the experimental (smooth curve) and simulated optical density profiles (a) before, (b) near, and (c) after stagnation. The profile of a uniform density sphere (diameter = 105 μm and C density = 25 g/cm³) is shown in each graph as reference (grey). The profiles were taken along a line through the center of the mass, perpendicular to the cone axis.

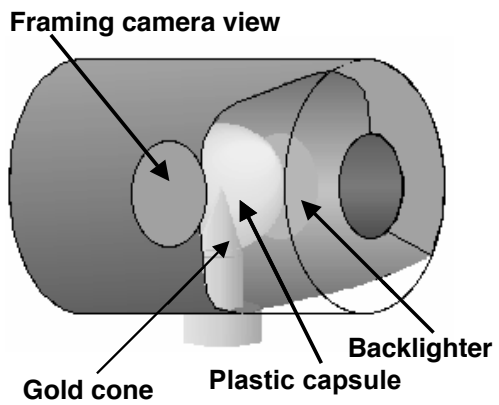
Figure 5. Full width at half absorption of profiles as a function of time for simulation and two experiments.

Figure 6. (a) Simulated and (b) experimental x-radiograph at stagnation. The simulation contains lines showing the original and deformed cone profile, and the maximum extent

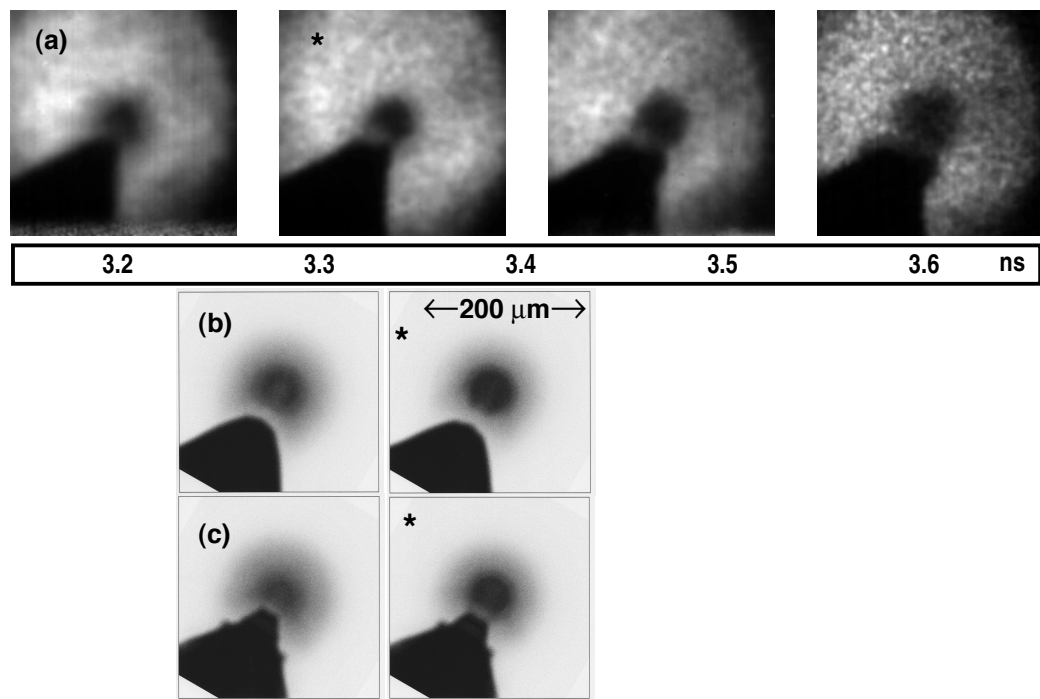
of gold vapor expansion, which occurred at an earlier time, ~ 2.6 ns. The experimental image uses a logarithmic grey scale to show the transmission through the gold vapor and has a white line marking the boundary of the deformed cone.



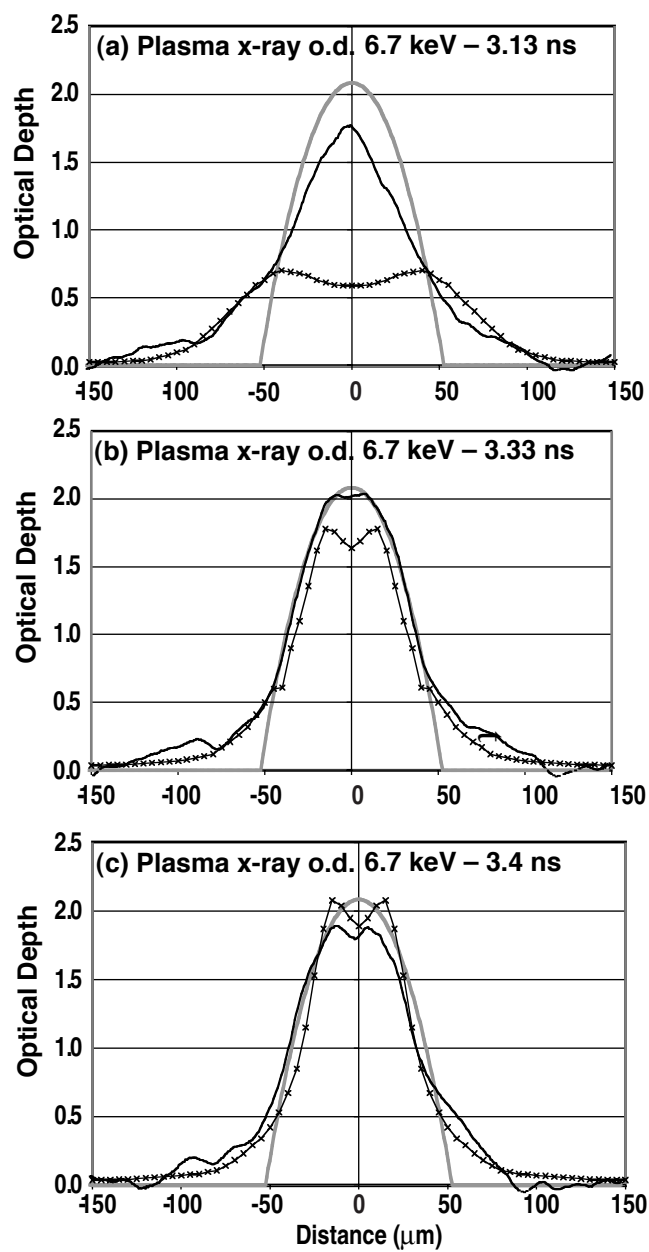
R.B. Stephens Figure 1



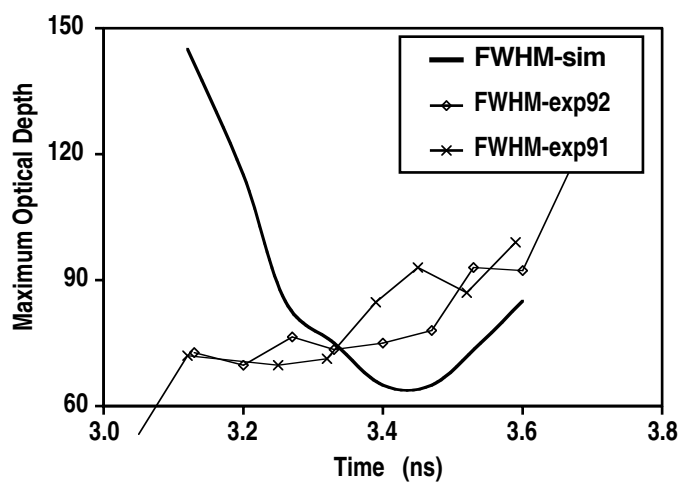
R.B. Stephens Figure 2



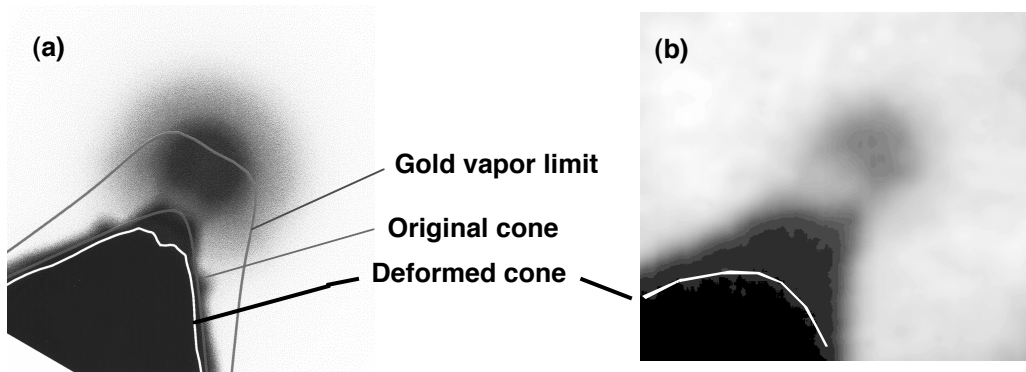
R.B. Stephens Figure 3



R.B. Stephens Figure 4



R.B. Stephens Figure 5



R.B. Stephens Figure 6